Microbiology (2015), **161**, 1034–1049 DOI 10.1099/mic.0.000072

Identification of antigen Ag43 in uropathogenic *Escherichia coli* Dr$^+$ strains and defining its role in the pathogenesis of urinary tract infections

Beata Zalewska-Piątek, Rafał Piątek, Marcin Olszewski and Józef Kur

Department of Molecular Biotechnology and Microbiology, Gdańsk University of Technology, ul. G. Narutowicza 11/12, 80-233 Gdańsk, Poland

Correspondence
Beata Zalewska-Piątek
beazalew@pg.gda.pl

Received 24 November 2014
Accepted 3 March 2015

Urinary tract infections (UTIs) caused by uropathogenic *Escherichia coli* (UPEC) are amongst the most common bacterial infectious diseases in the developed world. The urovirulence of UPEC is mainly associated with the surface-exposed fimbrial adhesins and adhesins of the autotransporter (AT) family. The best studied of these proteins is antigen Ag43 mediating cell aggregation, adhesion and biofilm development as the causes of chronic UTIs. The *E. coli* IH11128 Dr$^+$ (*dra* $^+$) strain of the Dr/Afa$^+$ family of adhesins possesses two major surface-exposed virulence factors: Dr fimbrial polyadhesin and DraD protein (fimbrial tip subunit or protein component of the adhesive sheath). Here, we identified for the first time, to our knowledge, the *agn43* gene encoding Ag43 in the WT clinical isolate of UPEC Dr$^+$ as a new virulence factor not yet tested. We also found that Dr fimbrial expression, which like Ag43 is under the control of a phase-variable mechanism, did not exclude Ag43 surface presentation. However, the presence of Dr fimbriae supported by other structures on the cell surface caused a physical neutralization of Ag43-mediated autoaggregation during *in vitro* growth. The fimbrial bundling further increased the distance between the adjacent Ag43$^+$ cells, thus preventing head-to-tail association between surface-exposed Ag43 subunits and their interactions with the host cells. The investigations showed that Ag43 did not act as a specific adhesin and invasin, conversely to the major virulence factors of *E. coli* Dr$^+$, but played significant roles in the viability and metabolic activity of bacterial cells forming biofilm, and in the survival of bacteria within invaded epithelial cells.

INTRODUCTION

Chronic and recurrent urinary tract infections (UTIs) are amongst the most common bacterial infectious diseases, affecting millions of humans in the developed world (Foxman, 1990). The major aetiological agents and causes of UTIs (65–90 % of cases) are strains of uropathogenic *Escherichia coli* (UPEC). UTIs usually start as bladder infections and then often reach the kidneys (Foxman, 2002; Foxman & Brown, 2003).

UPEC, as extra- and intracellular pathogens, have the ability to adhere to and invade many host cell types, facilitating the establishment of acute UTI as well as the recurrence of UTIs (Justice *et al.*, 2004). Several virulence factors of UPEC are associated with increased risk of UTIs. Amongst these virulence factors are adhesins that contribute to the colonization of the urinary tract (Johnson, 1991; Klemm & Schembri, 2000; Oelschlaeger *et al.*, 2002). The Dr/Afa$^+$ family of adhesins belongs to the third most common group of colonization factors of UPEC, behind type 1 and P pili (Nowicki *et al.*, 2001; Van Loy *et al.*, 2002; Servin, 2005; Le Bouguénec & Servin, 2006). *E. coli* strains expressing the Dr family of adhesins have a gestational tissue tropism; however, the Dr/DraE adhesins represent a key lethal factor in pregnant rats (Goluszko *et al.*, 1997a, b; Nowicki *et al.*, 1997, 1999; Fang *et al.*, 2001; Wróblewska-Seniuk *et al.*, 2005, 2011). Dr adhesins are also responsible for the risk of recurrent UTIs (Foxman *et al.*, 1995).

Dr haemagglutinin, like the other proteins of the Dr family, is encoded by a *dra* operon (*draA*, *draB*, *draC*, *draD*, *draP* and *draE*) with a similar genetic organization. The genes of the operon (under a phase-variable mechanism) are required for the biogenesis of Dr fimbriae (Nowicki *et al.*, 1989; van der Woude *et al.*, 1992; Piątek *et al.*, 2005). Dr fimbriae are homopolymeric structures composed of DraE subunits with the DraD tip subunit capping the fibre (Anderson *et al.*, 2004; Piątek *et al.*, 2005;

Abbreviations: AT, autotransporter; DAF, decay accelerating factor; EPS, exopolysaccharide; IFM, immunofluorescence microscopy; PAS, periodic acid–Schiff; PI, propidium iodide; TTC, 2,3,5-triphenyltetrazolium chloride; UTI, urinary tract infection; UPEC, uropathogenic *Escherichia coli*.

Zalewska *et al.*, 2005; Cota *et al.*, 2006; Zalewska-Piątek *et al.*, 2008). DraD protein can be expressed in two forms: fimbriae associated and fimbria non-associated (Zalewska *et al.*, 2005; Zalewska-Piątek *et al.*, 2008). These main virulence determinants of *E. coli* Dr$^+$ strains are responsible for adhesion to the receptors of host tissues or adhesion to abiotic surfaces, which is the first step of biofilm formation by the bacteria (Zalewska-Piątek *et al.*, 2008, 2009, 2013). The ability of the *E. coli* Dr$^+$ strain to adhere to a diverse range of surfaces is important for colonization, survival and persistence of the bacteria within the urinary tract. In addition to attachment to the colonized surface, Dr fimbriae can be involved in biofilm maturation (Zalewska-Piątek *et al.*, 2013). Development of large cell aggregates and biofilms, which are a significant barrier against microbial agents, can also be the cause of persistence and relapse of infection.

The second group of virulence factors associated with adhesion, aggregation and biofilm formation are autotransporter (AT) proteins of a large family of outer membrane/secreted proteins in Gram-negative bacteria (Henderson & Nataro, 2001; Henderson *et al.*, 2004; Kajava & Steven 2006; Celik *et al.*, 2012). The AT proteins are characterized by a specific domain architecture which consists of an N-terminal signal sequence, a passenger (α^{43}) domain anchored to the cell surface or released into the extracellular surrounding and a translocation (β) domain forming a β-barrel pore in the outer membrane (Henderson *et al.*, 2000, 2004; Henderson & Nataro, 2001).

The largest and most diverse group of the AT family are the AIDA-I-type AT proteins possessing common domain architecture characteristic of AT proteins (Wells *et al.*, 2010). The representative member of the AIDA-I type is the phase-variable surface-located adhesin antigen Ag43 best characterized in *E. coli* K-12 (Owen & Kaback, 1978; Henderson *et al.*, 1997). Ag43 from *E. coli* K-12 is connected with the early stages of biofilm formation (Schembri *et al.*, 2003). In this *E. coli* strain, the intercellular Ag43–Ag43 interactions responsible for bacterial autoaggregation and floculation of static liquid cultures are blocked by type 1 fimbriation (Diderichsen, 1980; Hasman *et al.*, 1999).

Ag43 was found in many non-pathogenic and pathogenic *E. coli*, including UPEC, in which it is associated with urovirulence (Anderson *et al.*, 2003; Ulett *et al.*, 2007). UPEC strains encode multiple copies of the *agn43* (*flu*) gene with the variations within the α domain determining the biological function of the Ag43 protein (Henderson & Nataro, 2001; Klemm *et al.*, 2004). The reference UPEC strain, CFT073, encodes two allelic variants of *agn43* (*agn43a*/*fluA*$_{CFT073}$ and *agn43b*/*fluB*$_{CFT073}$) and UTI89 possesses only one copy of the *agn43* (*agn43a*$_{UTI89}$) gene, connected with biofilm formation and long-term colonization of the mouse urinary tract. Generally, surface-exposed Ag43 in UPEC is responsible for the formation of intracellular biofilm-like communities in the murine bladder, which suggests its role in both abiotic biofilm formation and biofilm-like development in the host tissue (Anderson *et al.*, 2003; Ulett *et al.*, 2007).

Here, we identified for the first time, to our knowledge, the *agn43* gene in the WT clinical isolate of the UPEC IH11128 Dr$^+$ (*dra*$^+$) strain of the Dr/Afa$^+$ family of adhesins, demonstrating its significant roles in the viability and metabolic activity of bacterial cells forming biofilm, and in the survival of the bacteria within invaded epithelial cells. The investigations showed that Ag43 did not act as a specific adhesin and invasin, conversely to the major virulence factors of the *dra* operon, i.e. Dr fimbriae and DraD invasin. This is also the first report showing that, apart from DraE and DraD contributing to adhesion to both biotic and abiotic surfaces and invasion of the host cells, *E. coli* Dr$^+$ strains express another virulence factor such as antigen Ag43 playing a role in the pathogenesis of UTIs through the formation of an intracellular reservoir of bacterial aggregates. The local bacterial reservoirs could be the cause of the survival and persistence of *E. coli* Dr$^+$ strains within colonized epithelial cells. The data obtained also made it possible to propose a common model which can take place during the course of infection caused by Dr/Afa$^+$ *E. coli* strains.

METHODS

Bacterial strains, plasmids and reagents. The expression of genes encoded by the *dra* operon was carried out in *E. coli* IH11128 (Nowicki *et al.*, 1987) and IH11128/*agn43*$^-$ (this paper). *E. coli* IH11128 (Dr/Ag43$^+$) is a strain of clinical origin (isolated from a patient with pyelonephritis) bearing Dr fimbriae. *E. coli* IH11128/*agn43*$^-$ is an *agn43* mutant strain (with an *agn43* gene knockout) described here.

E. coli BL21(DE3) (Novagen) was used as a negative control of *agn43* gene expression. The strain is a λDE3 lysogen, which carries the gene for T7 RNA polymerase under *lacUV5* promoter control.

E. coli AAEC191A (a Δ*fim* strain) is a K-12 derivative strain, with a deletion of the entire *fim* operon (performed by allelic exchange) not expressing type 1 fimbriae (Blomfield *et al.*, 1991), and representing a reference strain to analyse production and cell aggregation mediated by Ag43. *E. coli* AAEC/*agn43*$^-$ is an *agn43* mutant strain (with an *agn43* gene knockout) described here and mainly used as a negative control of Ag43 surface exposition.

All bacterial *E. coli* strains (of laboratory or clinical origin) were grown on minimal medium, supplemented with the appropriate antibiotics (50 μg kanamycin ml^{-1} or 100 μg ampicillin ml^{-1}; Sigma) at 37 °C. The minimal medium used was M63 supplemented with 0.2 % glycerol, Casamino acids (1 %) and $FeSO_4$ (3 μM) (M63/CAA/Fe).

Polyvinylchloride (96-well, microtest flexible assay plates) or polystyrene plates (six-well assay plates) and glass coverslips were obtained from Becton Dickinson; 1 % 2,3,5-triphenyltetrazolium chloride (TTC), a dye used for measurement the metabolic activity of viable cells forming biofilm, and PBS tablets were purchased from Merck.

Antisera. Rabbit Ag43 antiserum directed against the α domain of Ag43 from K-12 was a gift from P. Owen (Microbiology Department, Myone Institute of Preventive Medicine, Trinity College, Dublin, Ireland). Rabbit anti-Dr antibodies raised against purified native Dr fimbriae were purchased from Immunolab. Anti-rabbit IgG

(whole-molecule) antibodies conjugated to horseradish peroxidase or FITC were purchased from Sigma.

Cell lines. HeLa cells were cultured in minimum essential medium (MEM) supplemented with 10 % (v/v) FBS (Sigma) and penicillin/streptomycin solution (Sigma) in a 5 % CO_2 atmosphere at 37 °C. The cell line was passaged using 0.25 % (v/v) trypsin containing EDTA (Sigma).

DNA analysis and TargeTron intron-mediated *agn43* gene disruption. The *agn43* gene of the various *E. coli* strains was first amplified using 30 cycles of PCR (94 °C for 30 s, 55 °C for 1 min and 72 °C for 3 min in a Biometra thermocycler) with primers for Agn43-for (5′-ATGAAACGACATCTGAATAC-3′) and Agn43-rev (5′-TCAGAAGGTCACATTCAGTG-3′). The 3120 bp PCR products were purified from the agarose gel bands (DNA Clean-UP kit; A&A Biotechnology) and digested with *Kpn*I endonuclease. The obtained restriction fragments were 1189 and 1193 bp in length. The sequence alignments of the *agn43* genes were generated based on GeneDoc and CLUSTAL_X software.

The *agn43* gene knockout was performed by insertion of the group II intron using the TargeTron GeneKnockout System according to the instructions of the manufacturer (Sigma). The modified group II intron (under the control of the T7 promoter) was inserted via the activity of a RNA–protein complex expressed from a pACD4K-C-loxP expression vector provided in the kit. pAR1219 was used as a source of the T7 RNA polymerase gene. The intron was mutated by PCR with primers designed based on the computer algorithm: IBS (5′-AAAAAAGCTTATAATTATCCTTAGGCACCGGAGCCGTGCGCCCAGATAGGGTG-3′), EBS2 (5′-TGAACGCAAGTTTCTAATTTCGATTGTGCCTCGATAGAGGAAAGTGTCT-3′) and EBS1d (5′-CAGATTGTACAAATCTGGTGATAACAGATAAGTCGGAGCCGTTAACTTACCTTTCTTTGT-3′). The kanamycin-resistant colonies were screened for *agn43* gene disruption by PCR with gene-specific primers (Agn43-for and Agn43-rev) flanking the insertion site and amplifying the entire inserted intron ($\sim$2 kb). Five bacterial colonies were the mutants. As a result 5120 bp length PCR products were obtained.

Immunofluorescence microscopy (IFM) of Ag43. Overnight bacterial cell cultures grown on M63/CAA/Fe at 37 °C for 24 h were centrifuged, washed gently and suspended in PBS. Bacterial suspensions (100 ml; 10^5–10^6 cells ml^{-1}) were incubated with a 1 : 500 dilution (Ag43 or Dr antisera) of the primary antibodies at 37 °C for 1 h. The reaction mixtures were then washed three times with PBS containing 10 % (v/v) glycerol and incubated with a 1 : 5000 dilution (anti-rabbit IgG-FITC conjugate) of secondary antibodies (37 °C for 1 h). Then, after three washes with PBS, the bacterial suspensions were loaded on glass slides and observed with an immunofluorescence microscope (Olympus BX-60).

Release of the α domain of Ag43. Bacterial cells from the overnight M63/CAA/Fe cultures were harvested by centrifugation and washed in 0.9 % (w/v) NaCl. The bacteria were then resuspended in 1 ml 75 mM NaCl and 0.5 mM Tris (pH 7.4). The α domain of Ag43 was released from the surface of bacterial cells by heating at 60 °C for 20 min. The cells were immediately cooled down, shaken (1 min) and centrifuged to separate the sheared outer proteins. The resultant Ag43 protein was precipitated overnight with 10 % acetone at 4 °C. Pellets were washed in 96 % ethanol, dried and resuspended in 100 µl Tris/EDTA buffer. Then, 15 µl each sample was separated by 15 % SDS-PAGE and stained with Coomassie Brilliant Blue R-250. Additionally, the whole-cell extracts (15 µl) of each *E. coli* strain were analysed by Western blotting with Ag43 antiserum.

Dr fimbriae purification. To isolate the fimbrial fractions, 100 ml M63/CAA/Fe medium (supplemented with ampicillin) was inoculated with single bacterial colonies scraped from the LA plates and grown with agitation at 37 °C for 24 h. Dr fimbriae were isolated by heat-shock treatment, ammonium sulfate precipitation and gel-filtration chromatography, as described previously (Zalewska *et al.*, 2003). Then, 15 µl samples were separated by 15 % SDS-PAGE, transferred onto nitrocellulose and analysed by Western blotting.

Western blot analysis. The samples were mixed with sample buffer and run in 15 % (w/v) polyacrylamide gels containing SDS. The proteins were electroblotted onto nitrocellulose membranes and incubated with anti-Ag43 antigen (analysis of the whole-cell lysates of *E. coli*) or anti-Dr adhesin antibodies (analysis of Dr fimbrial fractions) at a 1 : 5000 dilution, respectively. Blots were visualized according to Zalewska *et al.* (2003).

Electron microscopy of Dr fimbriae. Cells of the clinical *E. coli* IH11128 strain were grown on LA plates. A small portion of cells was scraped off a plate (with a platinum loop) and very gently suspended in a 10 µl drop of PBS. Carbon-coated copper grids (300 mesh) were floated on the cell suspensions for 1–2 min and then washed twice by being floated on 50 µl drops of PBS. They were then negatively stained with 1.5 % potassium phosphotungstate for 90 s. The preparations were analysed with a Philips CM 100 transmission electron microscope at 60 kV at an original magnification of $\times$3805.

Autoaggregation assay. To monitor autoaggregation differences of *E. coli* strains, overnight M63/CAA/Fe cultures were adjusted to OD_{600} 0.8 by dilution with the same medium and mixed vigorously before the start of the experiment. Aliquots of 3 ml culture were incubated in 5 ml standing tubes at room temperature. Then, 100 µl samples were taken 0.5–1 cm below the surface of the liquid, static cultures (at regular 30 min intervals) to measure OD_{595} (Victor3V plate reader; PerkinElmer).

Biofilm formation. Biofilm formation was analysed using the ability of bacterial cells grown on M63/CAA/Fe to adhere to the wells of 96-well microtitre plates, as described previously (Zalewska-Piątek *et al.*, 2009). After 48 h of static growth at 30 °C in the wells of the plates, the microbial biofilm formed from M63-grown cells was quantified using the TTC assay.

Biofilm quantification. Biofilm formation in microtitre plate wells was quantitatively determined by the TTC reduction method (Gabrielson *et al.*, 2002; McCluskey *et al.*, 2005). Prior to each assay, fresh 1 % TTC solution (in M63/CAA/Fe) was prepared and filter-sterilized through a 0.22 nm pore size filter. The biofilms were first washed two times with 200 µl PBS, and then 200 µl TTC (final concentration of 0.1 %) was added to each of the prewashed well and the control wells. The microtitre plate was then incubated in the dark for 5 h at 37 °C. Following incubation, 100 µl of each solution was transferred to new wells and the colour change was measured at 490 nm (Victor3V plate reader; PerkinElmer). The assay was performed in quadruplicate wells and repeated three times for each *E. coli* strain.

Viability of biofilm-forming cells. The viability of biofilm-forming cells of different *E. coli* strains was assessed by Fluo Cell Double Staining and Fluo Cell Counting kits according the manufacturer's instruction (MoBiTec). The bacterial cells were grown statically in the wells of six- or 96-well plates as described above. The biofilms were then washed two times with PBS and incubated with the prepared fluorescence assay solutions for 30 min at 37 °C. Finally, the fluorescence intensity was examined using a fluorescence microscope (Fluo Cell Double Staining kit) or fluorescence microplate reader (Fluo Cell Counting kit).

A Fluo Cell Double Staining kit was used for double staining of dead cells with propidium iodide (PI) and viable cells with Calcein generated from Calcein-AM by the cellular esterases. PI red and Calcein green fluorescence intensities were observed at 617 nm (excitation at

545 nm) and 515 nm (excitation at 490 nm), respectively. The cells were examined microscopically under a ×40 objective lens (Olympus CKX41).

A Fluo Cell Counting kit was utilized for the fluorometric detection and estimation of living cell numbers. The amount of Calcein fluorescent dye was directly proportional to the number of viable cells in a culture medium. The fluorescence intensity was measured at 515 nm (Victor3V plate reader; PerkinElmer). The viable cell number in a sample medium was determined on a basis of the calibration curve ($y=6.3051x+28839$) prepared by the use of solutions containing known numbers of viable cells of *E. coli* IH11128 strain.

Exopolysaccharide (EPS) periodic acid–Schiff (PAS) staining. Biofilm formation on the wells of six-well polystyrene plates supported by glass coverslips was studied. Cells grown for 24 h under static conditions in M63/CAA/Fe (37 °C) were diluted in fresh media (1 : 40) and grown statically for another 24 h at 30 °C in the wells of the plates. After fixation of the bacterial cells in 10 % neutral-buffered formalin, the EPS coverage of 24 h biofilms was determined by PAS staining (Sigma), according to the manufacturer's instructions. Following this, the coverslips were rinsed with deionized water, air-dried and examined microscopically under a ×40 objective lens (Olympus CKX41). PAS staining intensity was verified by photogrammetric scanning of the analysed images as described previously (Zalewska-Piątek *et al.*, 2013).

Adhesion assay. HeLa cells were seeded in six-well plates with glass coverslips, and grown for 24 h in MEM medium with 10 % FBS and antibiotic solution (37°, 5 % CO_2). Before the test was performed, the cells were washed twice with pre-warmed PBS and the cell culture medium was replaced with MEM without antibiotics, but supplemented with 1 % FBS and 0.5 % methyl α-D-mannopyranoside (Sigma). The bacterial strains to be tested were grown overnight at 37 °C in M63 medium. The cells were then pelleted and resuspended in PBS (OD_{600} 0.8). An aliquot of 25 µl of each bacterial strain suspension was added to the wells of the plate and incubated for 1.5 h at 37 °C with 5 % CO_2. After incubation, the cells were stained with Giemsa and analysed as reported previously (Zalewska-Piątek *et al.*, 2008). The amount of bacteria added to HeLa cells minus the amount in the washing fractions represented the amount on glass coverslips. The second six-well plate, not stained with Giemsa, was used for quantitative analysis. The number of bacterial c.f.u. was estimated by 10-fold serial dilutions in PBS, plating on L-agar and overnight incubation at 37 °C. The assay was performed in duplicate and repeated three times.

Invasion assay. Bacterial invasion into HeLa cells was tested by the gentamicin protection assay as described previously (Goluszko *et al.*, 1997a, b; Plançon *et al.*, 2003). HeLa cells were seeded in 12-well plates, and grown for 24 h in MEM medium with 10 % FBS and antibiotic solution at 37 °C in 5 % CO_2. Before the assay, the cells were washed three times with pre-warmed PBS, and then fresh culture medium supplemented with 1 % FBS and 0.5 % methyl α-D-mannopyranoside (Sigma) was added. The *E. coli* isolates were harvested from overnight cultures in M63 medium and resuspended in PBS (OD_{600} 0.4). After incubation for 3 h at 37 °C with 5 % CO_2, the bacterial suspensions were removed, and the cells were washed twice with fresh MEM medium containing gentamicin (200 µg ml^{-1}) and incubated in the same medium for an additional 1 h to kill the extracellular bacteria and select for the internalized bacteria. Then, the cells were washed twice with PBS and incubated for 20 min at room temperature with 1 ml lysis buffer (0.9 % NaCl/0.1 % SDS). The cellular lysates were serially diluted and bacterial numbers estimated as above. Additionally, except for the standard invasion assay as above, the infected cells were incubated with gentamicin for 2, 24, 48 or 72 h. Each assay was performed in triplicate wells and repeated twice for each *E. coli* strain.

RESULTS

agn43 gene knockout and immunological detection of the adhesin antigen Ag43

Multiple genome comparison analyses of the *agn43* genes of UPEC strains, including the prototype clinical UPEC CFT073 (pyelonephritis isolate) (Welch *et al.*, 2002) and UTI89 (cystitis isolate) (Chen *et al.*, 2006) strains, and the human gut-derived K-12 *E. coli* laboratory strain, MG1655 (Blattner *et al.*, 1997), were generated using GenDoc and CLUSTAL_X. In the CFT073 strain, two Ag43 proteins, Ag43a and Ag43b, were identified (Mobley *et al.*, 1990; Klemm *et al.*, 2004; Ulett *et al.*, 2007). However, only Ag43a displayed a strong aggregation phenotype and promoted significant biofilm growth, whereas Ag43b impaired initial colonization and did not affect later stages of bacterial infection (Danese *et al.*, 2000; Ulett *et al.*, 2007; van der Woude & Henderson, 2008). The surface-located α domain of the Ag43a and Ag43b proteins showed 81.7 and 78.4 % amino acid identity, respectively, compared with the K-12 Ag43 α domain (Klemm *et al.*, 2004). UTI89 strain contained only one type of Ag43 protein, which was associated with the development of intracellular biofilm-like communities resembling biofilm and contributing to chronic UTI (Anderson *et al.*, 2003; Chen *et al.*, 2006). The data obtained were used to design primers for amplification of the *agn43* gene in all of the analysed *E. coli* strains of clinical and laboratory origin.

Identification of the *agn43* gene, in the laboratory reference *E. coli* AAEC191A and clinical *E. coli* IH11128 strains, was determined by PCR amplification and restriction analyses of the amplification products. The amplification was performed with primers (Agn43-for and Agn43-rev) complementary to the 5′ and 3′ region of the *agn43* gene. Specific PCR products which flank a 3120 bp fragment of the *agn43* gene were obtained in the case of *E. coli* AAEC191A and IH11128 (data not shown).

To define the function of Ag43 in the pathogenesis of UPEC, the *agn43* gene disruptions of the clinical *E. coli* IH11128 and laboratory reference AAEC191A strains were performed by insertion of a group II RNA intron. The knockout of selected genes was based on the TargeTron Gene Knockout System (Sigma). This system enables the retargeting intron to insert efficiently into virtually desired DNA fragments (Frazier *et al.*, 2003; Zhong *et al.*, 2003; Perutka *et al.*, 2004).

To examine the surface localization of Ag43, immunofluorescence staining with Ag43 antiserum was used (Fig. 1). The laboratory reference strain of *E. coli* AAEC191A (Fig. 1b) and its Ag43 knockout mutant (Fig. 1d) were used as positive and negative controls of surface exposure of Ag43, respectively. The clinical *E. coli* IH11128 strain exhibited the presence of Ag43 protein (Fig. 1f) as compared with *E. coli* IH11128/*agn43*$^-$ in which the *agn43* gene disruption was created (Fig. 1h). The results confirmed the effectiveness of the *agn43* gene knockout in the *E. coli* strains.

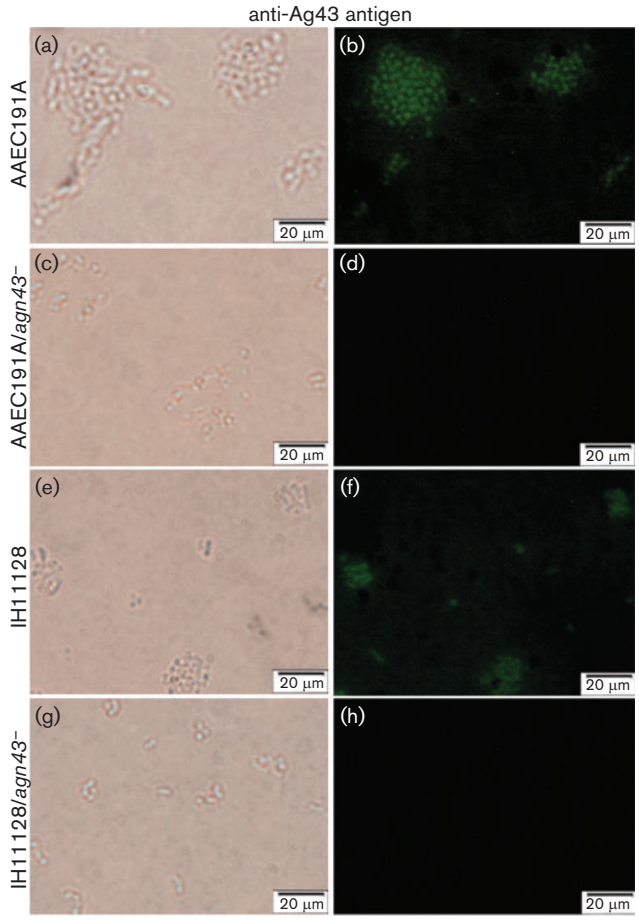

Fig. 1. Surface display of Ag43 of *E. coli* strains. Bacteria were incubated with Ag43 antiserum and FITC-coupled serum, and examined by IFM. Phase-contrast and IFM micrographs of *E. coli* strains (a, b) AAEC191A, (c, d) AAEC191A/*agn43*$^-$, (e, f) IH11128 and (g, h) IH11128/*agn43*$^-$. Bar, 20 μm.

The ability of *E. coli* AAEC191A and IH11128 strains to produce Ag43 protein was also confirmed by immunodetection using Ag43-specific antiserum (Fig. 2a, lanes 1 and 4). A faint bands corresponding to a low level of the Ag43 polyprotein precursor with the signal sequence (~100 kDa), consisting of two subunits α^{43} and β^{43} (molecular masses of 49.8 kDa and 51.5 kDa given in the literature, respectively) (Caffrey & Owen, 1989) and a surface-localized α domain were observed in the whole-cell lysates of the *E. coli* strains (reported molecular mass of 50–60 kDa). The faint immunological signal could be connected with a weak reactivity of the serum used. The same bands were absent in the *E. coli* AAEC191A/*agn43*$^-$ and IH11128/*agn43*$^-$ knockout mutant strains (Fig. 2a, lanes 2 and 3).

Release of the α domain of Ag43 and aggregation phenotype of the *E. coli* strains

In order to demonstrate the characteristic property of the Ag43 α domain associated with its release from the cell surface by heating to 60 °C, the clinical and laboratory reference *E. coli* strains were subjected to a brief heat treatment, centrifugation, purification by precipitation and SDS-PAGE analysis (Fig. 2b). Both of the Ag43 knockout mutant *E. coli* strains, IH11128/*agn43*$^-$ and AAEC191A/*agn43*$^-$, as well as *E. coli* BL21(DE3) (not encoding the *agn43* gene on the genome) used as the negative control (Fig. 2b, lanes 2, 4 and 5) did not show production of Ag43 protein and release the Ag43 α domain from the cell surface after heating the bacterial cells. The Ag43 α domain released from the cell surface was identified in the heat-extracted protein samples (bands corresponding to ~ 50 kDa) prepared from the cultures of WT *E. coli* IH11128 (Fig. 2b, lane 1), harbouring the whole *dra* operon, and the laboratory *E. coli* AAEC191A strain (Fig. 2b, lane 3), with the deletion of the *fim* operon. The examination of *E. coli* IH11128 also showed that Dr fimbriae expression had no effect on Ag43 surface exposure. The level of the isolated α domain was similar in the case of both studied *E. coli* strains. Dr fimbriae production at the bacterial cell surface of the WT IH11128 strain and its Ag43 knockout mutant was assayed by IFM and Western blot analysis with anti-Dr serum (Fig. 3a, b, lane 1). The *agn43* gene knockout did not influence the production of Dr fimbriae (Fig. 3a, b, lane 2). Additionally, electron microscopy revealed the bundling of Dr fimbriae on the surface of *E. coli* IH11128 Dr$^+$ (Fig. 3c), which increased the distance between bacterial cells. The fimbrial bundling could be sufficient to inhibit the Ag43–Ag43 interactions, thus abrogating cell autoaggregation, although we cannot exclude the role of other surface-located structures in this process.

To further examine this hypothesis, the *E. coli* strains of clinical and laboratory origin were subjected to an autoaggregation assay. The aggregation phenotype of Ag43 is localized to the α domain (Klemm *et al.*, 2004). The flocculation and settling profile in static liquid suspensions (referred to the initial OD_{595} and defined as 100 %) was observed only in the case of *E. coli* AAEC191A (a K-12 Ag43 derivative) overnight culture (86, 65, 46 and 30 % after 30, 60, 90 and 120 min, respectively). The *E. coli* AAEC191A/*agn43*$^-$ knockout strain lost the ability to form cell aggregates settling out of the suspension. The studies confirmed a conserved ability of Ag43 to mediate cell-to-cell aggregation and microcolony formation as a prelude to biofilm development. The clinical *E. coli* IH11128 and its Ag43 knockout mutant strain did not reveal the aggregation phenotype, which indicated that Dr fimbriae supported by other surface-exposed structures can physically block the close cell-to-cell contact required for Ag43-mediated cell aggregation. However, the results obtained did not exclude the role of Ag43 during the formation of intracellular bacterial aggregates after invading the colonized host cells.

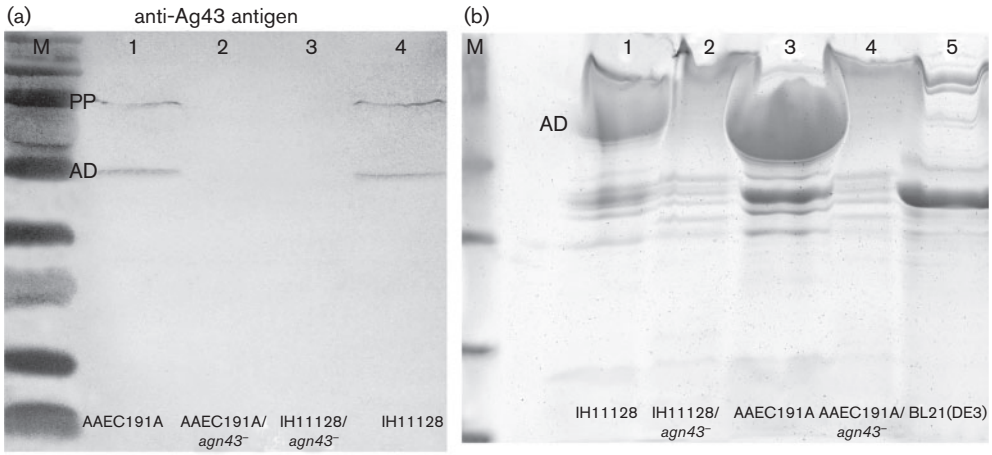

Fig. 2. (a) Immunofluorescence detection of Ag43 expression in *E. coli* strains. Western blot analysis of whole-cell lysates was performed using Ag43 antiserum that reacted with the Ag43 polyprotein precursor (PP) and α domain subunit (AD). Lane M, PageRuler Prestained Ladder Plus (Fermentas), with markers at 250, 130, 100, 70, 55, 35, 27, 15 and 10 kDa; lane 1, *E. coli* AAEC191A; lane 2, *E. coli* AAEC191A/*agn43*$^-$; lane 3 *E. coli* IH11128/*agn43*$^-$; lane 4 *E. coli* IH11128. (b) SDS-PAGE analysis of the Ag43 α domain subunit released from *E. coli*. Protein preparations were obtained by subjecting cells to brief heat treatment, centrifugation and precipitation. Lane M, Low Molecular Weight Calibration Kit (Amersham Pharmacia Biotech), with markers at 94.0, 67.0, 43.0, 20.1, and 14.4 kDa; lane 1, *E. coli* IH11128; lane 2 *E. coli* IH11128/*agn43*$^-$; lane 3 *E. coli* AAEC191A; lane 4, *E. coli* AAEC191A/*agn43*$^-$; lane 5 *E. coli* BL21(DE3)

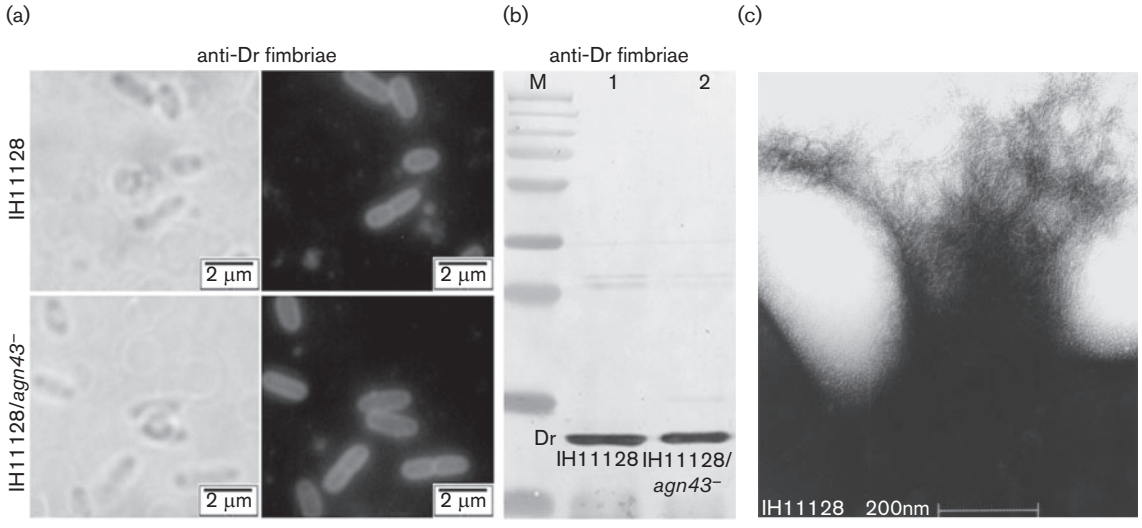

Fig. 3. Dr fimbriae surface expression in *E. coli* Dr$^+$ strains. (a) Surface display of Dr fimbriae examined by IFM. Bacteria were incubated with Dr antiserum and FITC-coupled serum. Phase-contrast and IFM micrographs of *E. coli* IH11128 and *E. coli* IH11128/*agn43*$^-$ are shown. Bar, 2 μm. (b) Western blot analysis of the fimbrial fractions isolated from the cellular surfaces performed using Dr antiserum and horseradish peroxidase-coupled serum. All samples were denatured at 98 °C, separated by 15 % SDS-PAGE and transferred onto nitrocellulose. Lane M, PageRuler Prestained Protein Ladder Plus (Fermentas), with markers at 250, 130, 100, 70, 55, 35, 27, 15 and 10 kDa; lanes 1 and 2, Dr appendage fractions of *E. coli* IH11128 and IH11128/*agn43*$^-$, respectively. (c) Electron micrograph of a negatively stained preparation of *E. coli* IH11128 harbouring the *dra* operon. Bar, 200 nm.

Biofilm formation and cell viability in biofilms assessed by TTC reduction and fluorescence staining of bacteria

Biofilm formation in microtitre plate wells was quantitatively determined by rapid TTC colorimetry. The TTC assay uses TTC dye, which is reduced to a water-soluble brown formazan salt product by the bacterial enzymes of the respiratory chain localized in the cytoplasmic membrane. The colorimetric change can be measured spectrophotometrically. The absorbance of the cell supernatant is proportional to the number of living and metabolically active microbial cells (Adam *et al.*, 2002; McCluskey *et al.*, 2005; Pettit *et al.*, 2005).

TTC reduction and biofilm development was observed in the case of the studied clinical *E. coli* IH11128 and IH11128/*agn43*$^-$ knockout mutant and laboratory reference *E. coli* AAEC191A strains. The assay also revealed differences in biofilm formation between the two groups of *E. coli* strains. The laboratory *E. coli* AAEC191A strain developed biofilm at the level of 0.227 (given as the mean absorbance value of three assays). However, its Ag43 and type 1 fimbriae-negative mutant strain was found to be defective in biofilm formation and not metabolically active. The results confirmed a conserved role of Ag43 not affected by fimbriation in bacterial aggregation and biofilm growth. The mean absorbance values determining the capacity of biofilm formation by the clinical *E. coli* IH11128 and its Ag43 mutant strain were 0.342 and 0.256, respectively. The enzymic activity of the *E. coli* IH11128/*agn43*$^-$ strain was compared with the WT clinical isolate for which the metabolic activity was determined as a 100 %. Therefore, in the case of the Ag43$^-$ mutant strain, we observed a 25 % reduction in metabolism, which may suggest a role for Ag43 in the viability of cells in the bacterial communities forming biofilm and exclude a role for Ag43 in the early steps of adhesion to the abiotic surface.

Further examination of the cell viability of *E. coli* strains forming biofilm was performed using microscopic and fluorometric detection. The bacterial cells were single (Fig. 4) or double stained with Calcein or PI and Calcein, respectively (Fig. 5). The double staining of each of the studied *E. coli* strains allowed fluorescence microscopy monitoring of viable and dead cells in biofilm by excitation of both fluorescent dyes. However, the single staining of bacteria was utilized for the fluorometric detection of living cell numbers. PI has the ability to pass through disordered areas of dead cell membranes and intercalates with the DNA, and Calcein produced from Calcein-AM is able to permeate through the viable cell membranes into the cytoplasm. PI emitted a strong red fluorescence only in dead cells (Fig. 5b, e, h, k) and Calcein green fluorescence only in viable cells (Fig. 5c, f, i, l).

E. coli AAEC191A/*agn43*$^-$ was used as a negative control of biofilm formation in both types of experiments (Figs 4b and 5e, f) in comparison with *E. coli* AAEC191A representing the ability to produce Ag43 and thus biofilm development (Figs 4a and 5b, c). The green fluorescence intensity emitted by *E. coli* AAEC191A/*agn43*$^-$ was very low and poorly detectable (Fig. 5f). IFM of WT *E. coli* IH11128 revealed the presence of viable cells (green fluorescence) (Fig. 5i) and a reduced number of dead cells in biofilm (only single bacterial cells emitting red fluorescence were visible) (Fig. 5h) compared with its Ag43$^-$ mutant. *E. coli* IH11128/*agn43*$^-$ showed an increased amount of dead cells (Fig. 5k) and a decreased number of viable cells (Fig. 5l) after staining with PI and Calcein, respectively. The same results were obtained after double and single staining of bacterial cells in biofilm analysed by IFM or spectrophotometric measurements, respectively. Additionally, in the case of the Ag43$^-$ mutant of *E. coli* Dr$^+$, we could also observe clumps of cells forming microcolonies with a lower density compared with those of the WT strain. The results obtained coincide with the database on metabolic activity of the bacterial cells in biofilms of the *E. coli* Ag43$^-$ mutants and suggest a role for Ag43 in the survival of bacteria when they form a biofilm.

Detection of biofilm EPS by PAS staining

EPS production during biofilm formation was detected by PAS staining – a procedure used routinely for demonstrating glycol-containing cellular components (Fig. 6). First, the periodic acid oxidizes glycols to aldehydes and then Schiff's reagent creates purple/magenta regions containing clumps of bacterial cells in a biofilm.

Microscopic examination of PAS staining of the studied *E. coli* strains revealed the production of extracellular matrix associated with biofilm development by the clinical *E. coli* IH11128 strain with the *agn43* gene disruption (Fig. 6d) and the laboratory *E. coli* AAEC191A strain with a deletion of type 1 fimbriae (Fig. 6a). The studies also confirmed EPS production by the *E. coli* IH11128 WT strain as described previously (Zalewska-Piątek *et al.*, 2013). In the native *E. coli* strain harbouring the whole genetic machinery required for Dr fimbriae biogenesis, EPS coverage of the biofilm was observed as the less intensely stained PAS areas (Fig. 6c). The observed effect was manifested by the reduced ability of the *E. coli* Dr$^+$ cells to mediate autoaggregation relative to the *E. coli* strains expressing only the DraD protein on the cell surface (Zalewska-Piątek *et al.*, 2013). The Ag43-deficient mutant of *E. coli*, IH11128/*agn43*$^-$ (Fig. 6d), demonstrated a similar level of EPS production as that of the WT IH11128. These data could also confirm the earlier supposition that the surface expression of Dr fimbriae blocks Ag43-mediated aggregation. The results obtained also revealed the role of Dr fimbriae at the first stages of biofilm development by stabilizing the cellular interactions and cell-to-surface attachment of the colonized surface. The laboratory *E. coli* AAEC191A/*agn43*$^-$ strain (Fig. 6b), without the ability to produce biofilm formation factors, such as Ag43 and type 1 fimbriae, was not stained with PAS compared with the *E. coli* AAEC191A strain expressing only the

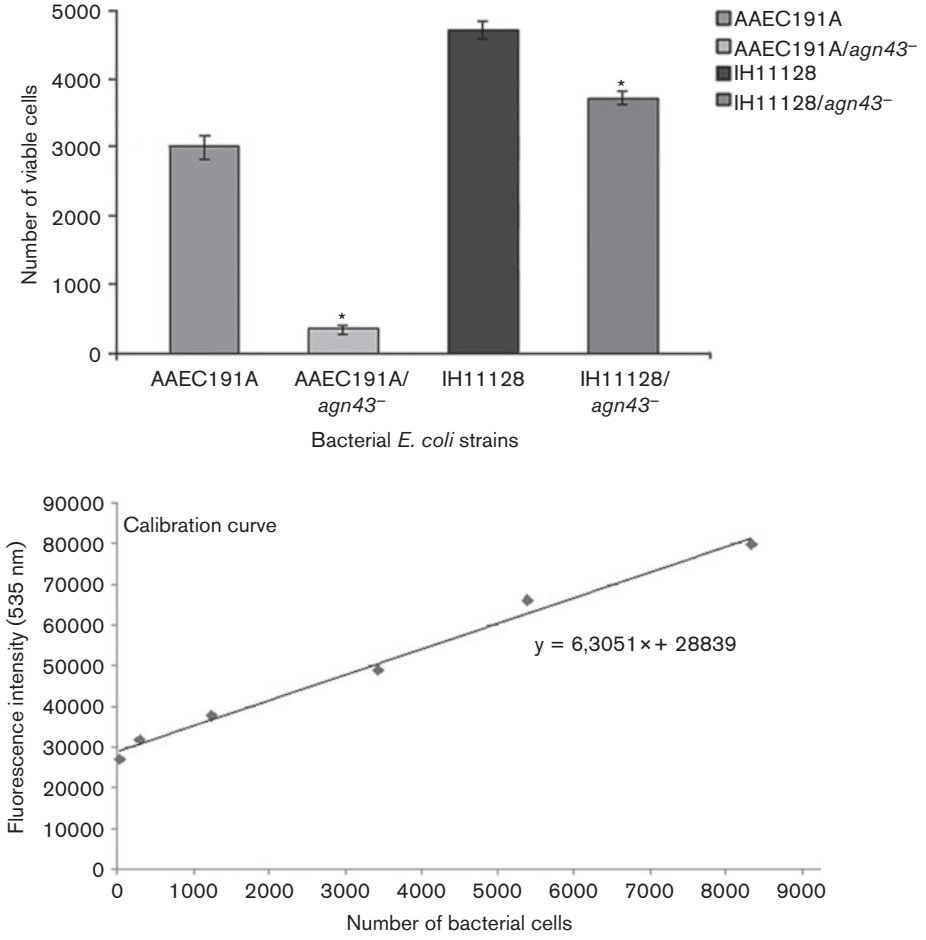

Fig. 4. Fluorometric detection of living cell numbers of *E. coli* strains forming biofilm: AAEC191A, AAEC191A/*agn43*$^-$, IH11128 and IH11128/*agn43*$^-$. Biofilms were grown in microtitre plate wells and stained with Calcein fluorescent dye. The green fluorescence intensity for each strain of *E. coli* was determined at 535 nm. The viable cell numbers in the samples were estimated on the basis of the calibration curve. Values represent mean ± SD of three independent experiments. The *agn43* gene knockout led to a significant reduction in the number of viable cells of the AAEC191A/*agn43*$^-$ and IH11128/*agn43*$^-$ strains compared with the viability of the control strains AAEC and IH11128 (*P<0.05 for each strain, as determined by Student's *t*-test).

Ag43 protein. Furthermore, the PAS-stained EPS matrix of the laboratory *E. coli* AAEC191A strain (Fig. 6a) was observed as more extensive purple areas containing large aggregates of clumping cells than those observed in the WT *E. coli* Dr$^+$ strains and its knockout mutant (Fig. 6c, d). However, the intensity of staining did not show a significant difference between the strains. The results could be connected with the autoaggregation phenotype of the laboratory *E. coli* strain not affected by the surface exposition of fimbrial structures.

Binding patterns of *E. coli* strains expressing Ag43

A HeLa cell adhesion assay was performed to examine the adherence patterns of the *E. coli* strains with and without the *agn43* gene disruption and estimate the contribution of adhesin antigen Ag43 to adherence (Fig. 7). The HeLa cell line was chosen because of its expression of DAF (decay accelerating factor) and lack of professional phagocytic properties. Another reason for selecting HeLa cells was associated with the anatomical site of origin, i.e. the cervix. The lower urogenital tract is a primary target of *E. coli* colonization preceding ascending UTI. Bound bacterial cells were stained with Giemsa. Bacterial numbers were estimated by serial dilutions and plating on L-agar. The laboratory *E. coli* AAEC191A/*agn43*$^-$ knockout strain was used as a negative control of adherence to HeLa cells because it had almost totally lost the adhesive properties (Fig. 7b). However, the laboratory *E. coli* AAEC191A strain with Ag43 surface expression showed localized adherence, although mostly the bacterial cells were not in direct contact with the epithelial cells of the HeLa cell line, but bound to each other (Fig. 7a). Those

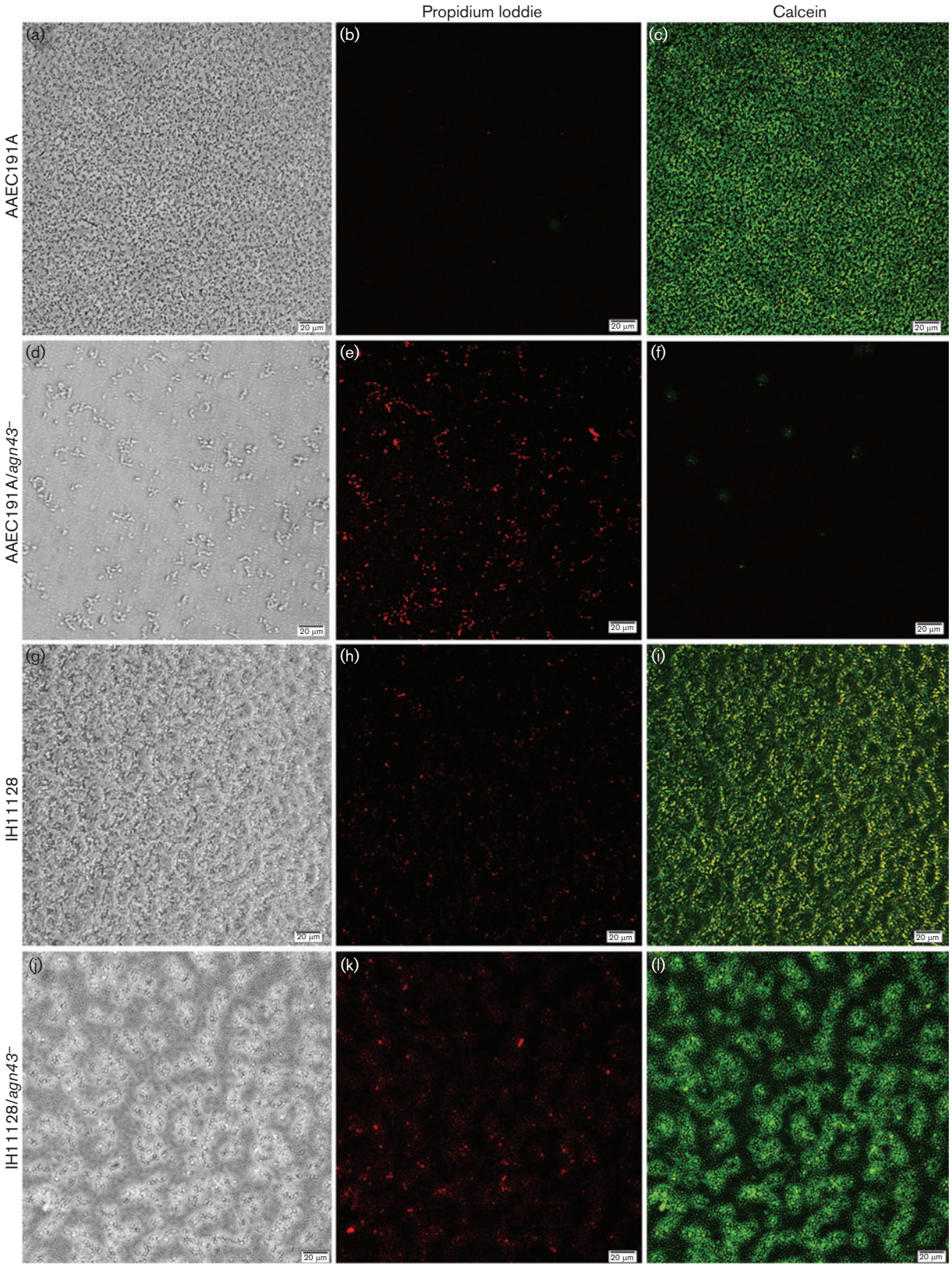

Fig. 5. Fluorescence staining of viable and dead cells in biofilms of *E. coli* strains. Biofilm-forming cells were grown in microtitre plate wells, incubated with a fluorescence solution of PI and Calcein, and examined by IFM. Phase-contrast and IFM micrographs of *E. coli* strains (a–c) AAEC191A, (d–f) AAEC191A/*agn43* $^{-}$, (g–i) IH11128 and (j–l) IH11128/*agn43* $^{-}$. Micrographs show PI (b, e, h, k) and Calcein (c, f, i, l) IFM of the bacterial cells, respectively. Bar, 20 µm.

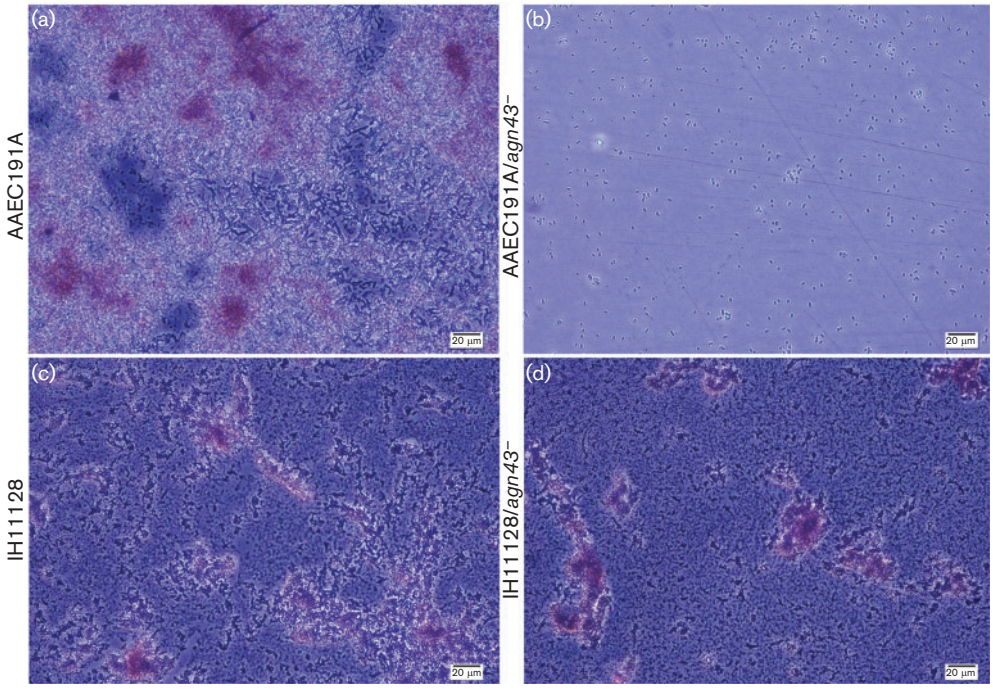

Fig. 6. Determination of EPS coverage of *E. coli* strains: (a) AAEC191A, (b) AAEC191A/*agn43*$^-$, (c) IH11128 and (d) IH11128/*agn43*$^-$. Bacterial cells were grown on glass slides, fixed, stained with PAS and examined by light microscopy. The images of several biofilms were examined in multiple regions and representative images are shown. The magenta regions represent the EPS coverage of the biofilm. Bar, 20 μm.

bound bacterial cells constituted the total number of attached bacteria. The experiments conducted with the cultures of *E. coli* IH11128 and its Ag43 knockout mutant, harbouring the *dra* operon, in both cases displayed the same strict adhesion phenotype to the cellular receptors, confirming the role of Dr fimbriae independently on Ag43 expression in adherence to epithelial cells (Fig. 7c, d).

To better understand the role of Ag43 as a new virulence factor, apart from Dr fimbriae and DraD protein, in the infectious process *in vivo*, the potential ability of the WT *E. coli* IH11128 Dr$^+$ and its Ag43$^-$ mutant strain to invade epithelial cells of HeLa was evaluated. The standard gentamicin protection assay was used. Gentamicin is not able to kill intracellular invasive bacteria; however, extracellular adhesive bacteria are eliminated. All analysed *E. coli* strains did not grow on L-agar plates after 1 h incubation in MEM with gentamicin. The bacterial internalization into HeLa cells was evaluated as the number of recovered colonies per well. The internalization rates of both the Dr$^+$ and Ag43$^+$ IH11128 strain and its Dr$^+$ and Ag43$^-$ strain were observed at a similar level of 10^5 c.f.u. ml^{-1}. The laboratory AAEC191A *E. coli* strain was able to invade HeLa cells at a low level of 10^1 c.f.u. ml^{-1} as opposed to its Ag43 mutant, which totally lost the invasive capacity. The results suggested that Ag43 does not play a role of a specific invasin. However, Dr fimbriae are crucial in the adherence and internalization of bacteria, and contribute to virulence by promoting the specific interactions with the cellular receptors and initial phase of colonization of the host tissues.

To finally define the role of Ag43 in virulence of the WT clinical isolate of *E. coli* Dr$^+$ and its Ag43$^-$ mutant, the number of viable bacteria cells was evaluated after different times of exposure to gentamicin (Fig. 8). The studies allowed us to determine the number of intracellular bacteria after a standard 3 h infection period, followed by 2, 24, 48 and 72 h of gentamicin treatment. The number of viable intracellular bacteria of the *E. coli* IH11128 Dr$^+$ strain decreased in the periods 2–24 and 24–48 h (defined as 58 and 30 %, respectively), and remained stable until 72 h and was at a level of 25 %. Intracellular survival of the *E. coli* IH11128/*agn43*$^-$ mutant dramatically decreased between 2 and 24 h, and survival of the bacteria was 7 % relative to that measured 2 h post-infection. No intracellular Ag43$^-$ bacteria were detected after 48 and 72 h. The results suggested that Ag43 is expressed *in vivo* during the formation of intracellular bacterial aggregates, contributing to the survival of bacteria within the colonized cells.

DISCUSSION

UTIs are amongst the most relevant infectious diseases worldwide, with chronic and recurrent courses (Foxman, 1990). Most UTIs are caused by UPEC strains categorized as extra- and intracellular pathogens (Foxman, 2002;

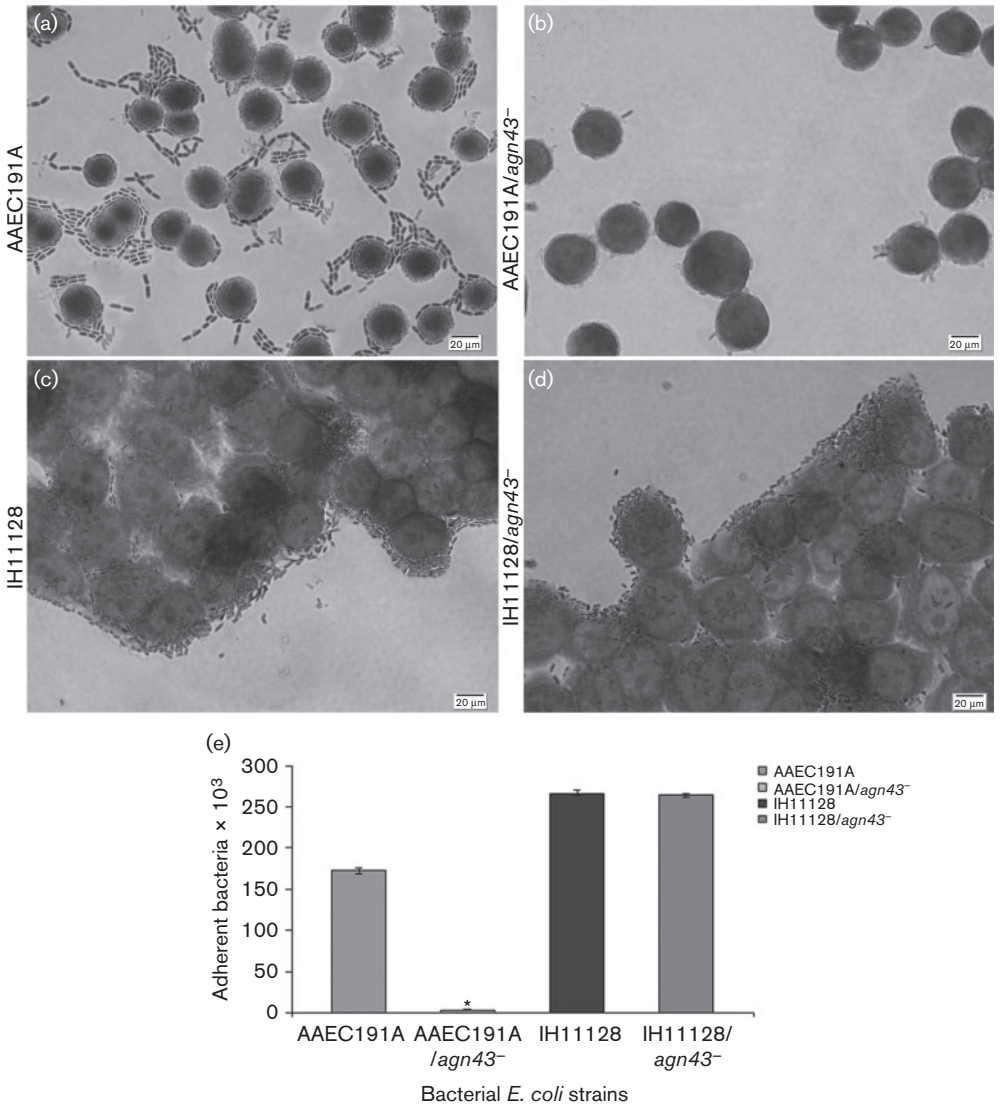

Fig. 7. Adherence of *E. coli* strains to HeLa. Bacterial strains were bound to HeLa cells, fixed, stained with Giemsa and examined by light microscopy: (a) AAEC191A, (b) AAEC191A/*agn43* $^{-}$, (c) IH11128 and (d) IH11128/*agn43* $^{-}$. Bar, 20 µm. (e) The attachment of *E. coli* to HeLa cells presented in the form of a bar graph was quantified by serial dilutions and plating on L-agar plates. Values represent mean ± SD of three independent experiments. The *agn43* gene knockout led to a significant reduction in the number of adherent AAEC191A/*agn43* $^{-}$ bacteria compared with the adherence mediated by the control strain AAEC191A (*P<0.05 for each strain, as determined by Student's *t*-test). IH11128 and IH11128/*agn43* $^{-}$ strains did not exhibit statistically significant differences.

Foxman & Brown, 2003; Justice *et al.*, 2004). UPEC have the ability to produce a great variety of fimbrial adhesins which contribute to the virulence and persistence of bacteria within the colonized urinary tract (Johnson, 1991). Adhesion to the host tissues is the first step of bacterial colonization. In addition to adhesion, UPEC are also able to invade a number of host cell types. Once internalized in the host urothelial cells, UPEC are trafficked into late endosomal compartments forming reservoirs that allow the intracellular persistence of bacteria (Mulvey *et al.*, 2001; Eto *et al.*, 2006; Mysorekar & Hultgren, 2006; Rana *et al.*, 2014).

UPEC Dr $^{+}$ strains, carrying the entire *dra* operon required for Dr fimbriae biogenesis, belong to the third most common group of uropathogenic bacteria (behind *E. coli pap* $^{+}$ and *fim* $^{+}$) (Nowicki *et al.*, 2001; Van Loy *et al.*, 2002; Servin 2005; Le Bouguénec & Servin, 2006).

In addition to the most intensively studied fimbrial adhesins such as Dr fimbriae, type 1 and P pili, UPEC are also able to produce non-fimbrial adhesins, including the AIDA-I-type AT proteins. The AT family represents a novel group of putative virulence factors whose functional

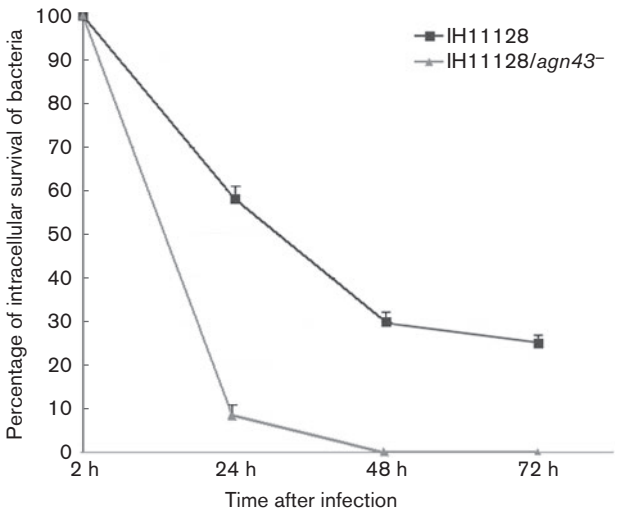

Fig. 8. Examination of intracellular survival of *E. coli* strains IH11128 and IH11128/*agn43*$^-$ in HeLa cells *in vitro*. The number of surviving intracellular bacteria was evaluated after various times of gentamicin treatment and is given as the percentage of that measured 2 h post-infection. Each point is the mean ± SD of at least two assays.

properties are linked to adhesion, aggregation and biofilm formation (Celik *et al.*, 2012; Henderson & Nataro, 2001; Henderson *et al.*, 2004; Kajava & Steven, 2006). The proteins are very well studied in many Gram-negative pathogens, except for UPEC. The prototype AT protein in UPEC is Ag43 that enhances bacterial virulence by promoting the development of intracellular biofilm-like communities and biofilm in UTI89 and CFT073 reference strains, respectively.

Here, we characterized Ag43 of the clinical UPEC IH11128 Dr$^+$ strain as a new virulence factor not yet tested, showing its role in the viability of bacterial cells forming biofilm and, after internalization of bacteria, their persistence inside epithelial cells. To determine the function of Ag43 in *E. coli* Dr$^+$ we focused on the clinical isolate IH11128 (with the functional *dra* operon) and laboratory reference *E. coli* AAEC191A strain (in which the *fim* operon was deleted), and the Ag43 knockout mutant strains.

Surface exposure of Ag43 of *E. coli* IH11128 strain analysed by Western blotting and IFM showed that Dr fimbrial and Ag43 expression are independent processes. Thus, the overexpression of Dr fimbriae also did not affect the amount of Ag43 isolated from the cell surface of the Dr/Ag43$^+$ clinical isolate.

Further studies were focused on blocking the bacterial autoaggregation phenotype by fimbriation. Thus, the culture of AAEC191A Ag43$^+$ cells not affected by fimbriation readily autoaggregated; however, disruption of the *agn43* gene abolished this property. In WT UPEC Dr/Ag43$^+$ and its Ag43$^-$ mutant, the Ag43–Ag43 interactions were abrogated by the physical presence of cell-surface-exposed Dr fimbriae or other cellular structures. Electron microscopy of the surface of *E. coli* Dr$^+$ cells additionally revealed fimbriae bundling, which could be responsible for increasing the distance between adjacent Ag43$^+$ cells. Taken together, our results were consistent with other investigations showing that the autoaggregation phenotype mediated by Ag43 is affected by large surface structures such as fimbriae, flagella and LPS (Hasman *et al.*, 1999; Schembri & Klemm, 2001; Sherlock *et al.*, 2004). Therefore, the role of Ag43 may not be associated with the first steps of bacterial adhesion and colonization, but with the formation of intracellular bacterial aggregates after invading the colonized host cells.

Further examinations were concentrated on studies of biofilm development and the adhesive/invasive phenotype of *E. coli* Dr/Ag43$^+$, *E. coli* Ag43$^+$ and the Ag43-defective mutant strains in order to determine the role of Ag43 in the survival of bacteria within epithelial cells.

Our previous investigations demonstrated the ability of *E. coli* Dr$^+$ strains with the *dra* operon, encoding the major virulence factors, i.e. Dr fimbriae and DraD protein, to form biofilm on abiotic surfaces under different nutritional conditions. The bacteria developing biofilm were surrounded by a polysaccharide matrix, as a major component of bacterial biofilms, specifically stained by PAS (Zalewska-Piątek *et al.*, 2013). Here, we demonstrated that the intensity of PAS staining of the clinical *E. coli* Dr/Ag43$^+$ and its Ag43$^-$ mutant strain did not show differences in EPS production. On the contrary, PAS staining of the laboratory reference *E. coli* AAEC191A Ag43$^+$ strain revealed the ability of bacteria to form large aggregates of clumping cells secreting EPS visualized by extensive purple areas. The observed effect could be connected with Ag43–Ag43 interactions mediating cell aggregation. The results also showed that Dr fimbriae in WT UPEC Dr$^+$ may play a role in EPS secretion as well as in both initial adherence by stabilizing the cell-to-cell and cell-to-surface interactions and microcolony formation.

We utilized TTC reduction to discriminate between living and dead cells in a biofilm formed in a microtitre plate system by the strains of *E. coli* with the *agn43* gene knockout and determine the role of Ag43 in this process (Gabrielson *et al.*, 2002; McCluskey *et al.*, 2005). The assay reflected differences in TTC activities between the strains of *E. coli* of clinical and laboratory origin. Clinical *E. coli* IH11128 Dr$^+$ strains with or without the *agn43* gene disruption possessed a greater ability to form biofilm than the laboratory *E. coli* Ag43$^+$/*fim*$^-$ strain compared with its Ag43$^-$ mutant, which showed no metabolic activity. The enzymic activity of the *E. coli* IH11128/*agn43*$^-$ strain was reduced by ~25 % compared with the WT UPEC Dr$^+$ strain. Thus, the cause of alterations in TTC metabolism by bacterial cells in a biofilm of each of the Ag43$^-$ mutants could be connected with the surface-associated changes. The surface differences probably arose from the absence of Ag43 short non-organelle-type adhesins

that protrude ~10 nm from the surface of bacterial cells (Kajava *et al.*, 2001). The TTC results were in agreement with single (Calcein) and double (PI and Calcein) fluorescence staining of each of the *E. coli* strains that developed biofilm. The *E. coli* IH11128/*agn43*$^-$ strain allowed the observation of a 20 % reduction in the number of viable bacterial cells. The results obtained also confirmed the role of Dr fimbriae in the early stages of biofilm formation and Ag43 in late stages after initial colonization, including increased survival of metabolically active bacterial cells within the microcolonies formed.

Finally, we analysed the adhesive and invasive phenotype of the WT UPEC Dr$^+$ and its Ag43-defective mutant strain. The adhesive phenotype of the clinical isolates was referenced to the laboratory *E. coli* AAEC191A/Ag43$^+$ strain. Ag43 antigen has been reported to mediate a low level of adhesion to certain mammalian cells (Owen *et al.*, 1996). Thus, the observed strength of binding of Ag43–Ag43-mediated cell interactions is very low and the Ag43$^+$ cells are also easily dispersed in comparison with the adhesion mediated by the fimbrial adhesins. In the case of the *E. coli* IH11128/*agn43*$^-$ mutant strain, we observed microscopically the same strict adhesion pattern of Dr fimbriae surrounding the HeLa cells as for the WT Dr$^+$ isolate as described previously (Zalewska-Piątek *et al.*, 2008). Thus, *agn43* gene disruption did not influence the interaction of the *E. coli* strain expressing Dr fimbriae on the cell surface with the host cellular receptors. However, the adherence pattern of the reference *E. coli* AAEC191A Ag43$^+$ strain not abrogated by fimbriation was quite different. The binding pattern mediated by the *E. coli* Ag43$^+$ strain was determined as a localized adherence strictly associated with Ag43$^+$ cellular interactions mediated via head-to-tail association between Ag43 subunits on the surface of adjacent bacterial cells. Therefore, many Ag43$^+$ cells forming aggregates on the surface of HeLa cells were not attached directly to HeLa cells. The data indicate that Ag43 does not play a role as a significant adherence molecule and Dr fimbriae are the major adhesive factors of the WT IH11128 Dr$^+$ strain required for the initial step of bacterial adhesion. Our observations are consistent with the previous results showing that the insertional Dr$^-$ mutant of the clinical *E. coli* IH11128 strain is less adherent and invasive (Goluszko *et al.*, 1997b).

We used the standard gentamicin protection assay to analyse the invasive properties of each of the *E. coli* strains. We demonstrated that the internalization of the laboratory *E. coli* Ag43$^+$ strain into HeLa cells was at a very low level (10^1 c.f.u. ml^{-1}). The same strain with the *agn43* gene knockout lost the invasive capacity. The WT UPEC Dr$^+$ and its Ag43-defective mutant strain showed internalization at a similar level of 10^5 c.f.u. ml^{-1}. These data are consistent with earlier investigations demonstrating that the adhesive and invasive abilities of both types of UPEC (Dr/Ag43$^+$ and Dr$^+$ with the *agn43* gene knockout) are dependent on two major virulence factors, i.e. Dr/DraE and DraD proteins (Goluszko *et al.*, 1997a, b, 2001; Jouve *et al.*, 1997; Nowicki *et al.*, 1988, 2001; Garcia *et al.*, 2000; Plançon *et al.*, 2003; Zalewska-Piątek *et al.*, 2008). Thus, the newly characterized Ag43 does not act as a specific adhesin and invasin, but the protein can hypothetically contribute to persistence of *E. coli* within the internalized cells.

To investigate our hypothesis, we analysed the fate of the internalized *E. coli* IH11128 and IH11128/*agn43*$^-$ strains at different times post-infection. The WT UPEC Dr$^+$ viable bacteria were maintained living within epithelial cells for 72 h. The persistent bacteria can form a reservoir in the epithelial cells required for further infection cycles. In the case of the Ag43$^-$ mutant of *E. coli* Dr$^+$, during 24 h we observed 7 % survival of the internalized bacteria and during 48–72 h we observed a total absence of live intracellular bacteria. The data highlight the importance of Ag43 protein in the survival and enhanced virulence of *E. coli* Dr$^+$ within epithelial cells.

In the view of these results, we hypothesized the common model of the course of UTI caused by the clinical strains bearing Dr and Afa-III adhesins of Dr/Afa$^+$ *E. coli* strains due to high-level homology between both adhesins. The bacterial colonization of the urinary tract *in vivo* into uroepithelial cells is associated with environmental and biological factors that could modulate the expression of Dra/AfaE and Dra/AfaD, and Ag43 as the third important virulence factor not previously identified in Dr/Afa$^+$ *E. coli* strains. The process of colonization consists of two steps: adhesion and invasion mediated by Dra/AfaE and Dra/AfaD with DAF and β_1-integrin as the receptors. It was suggested previously that Dra/AfaD can mediate the internalization process of Dr/Afa$^+$ *E. coli* using β_1-integrin (Plançon *et al.*, 2003). Further investigations are required to define the precise role of Dra/AfaD of the Dra/AfaE$^-$ mutants in the infectious process. The genes of the *dra/afa* operon are regulated by the phase-variation mechanism; thus, once internalized, bacteria after adaptation to a niche environment can be in a phase that switches the fimbrial expression from phase 'on' to 'off'. Under such conditions, it is possible to express the *agn43* gene encoding the Ag43 protein responsible for the formation of intracellular bacterial aggregates and biofilm development, increasing the persistence and survival of bacteria within the urinary tract. The observations are consistent with previous data showing that the tissue infection rate in the uteri of animals infected with the double AfaE$^-$AfaD$^-$ mutant was similar to the rate of those infected with single AfaE$^+$AfaD$^-$ and AfaE$^-$AfaD$^+$ mutants. The results may suggest that pregnant rats are not able to eliminate *E. coli* even not bearing both major virulence factors (Wróblewska-Seniuk *et al.*, 2011). Hypothetically, the explanation of the observed effect can be associated with the expression of *agn43* gene by the clinical Dr/Afa$^+$ *E. coli* that has not been recognized until now. Further examinations are needed to determine the direct role of Ag43 in the survival and persistence mechanisms of the internalized bacteria within the urinary epithelium.

REFERENCES

Adam, B., Baillie, G. S. & Douglas, L. J. (2002). Mixed species biofilms of *Candida albicans* and *Staphylococcus epidermidis*. *J Med Microbiol* **51**, 344–349.

Anderson, G. G., Palermo, J. J., Schilling, J. D., Roth, R., Heuser, J. & Hultgren, S. J. (2003). Intracellular bacterial biofilm-like pods in urinary tract infections. *Science* **301**, 105–107.

Anderson, K. L., Billington, J., Pettigrew, D., Cota, E., Simpson, P., Roversi, P., Chen, H. A., Urvil, P., du Merle, L. & Barlow, P. N. (2004). An atomic resolution model for assembly, architecture, and function of the Dr adhesins. *Mol Cell* **15**, 647–657.

Blattner, F. R., Plunkett, G. III, Bloch, C. A., Perna, N. T., Burland, V., Riley, M., Collado-Vides, J., Glasner, J. D., Rode, C. K. & other authors (1997). The complete genome sequence of *Escherichia coli* K-12. *Science* **277**, 1453–1462.

Blomfield, I. C., McClain, M. S., Princ, J. A., Calie, P. J. & Eisenstein, B. I. (1991). Type 1 fimbriation and *fimE* mutants of *Escherichia coli* K-12. *J Bacteriol* **173**, 5298–5307.

Caffrey, P. & Owen, P. (1989). Purification and N-terminal sequence of the alpha subunit of antigen 43, a unique protein complex associated with the outer membrane of *Escherichia coli*. *J Bacteriol* **171**, 3634–3640.

Celik, N., Webb, C. T., Leyton, D. L., Holt, K. E., Heinz, E., Gorrell, R., Kwok, T., Naderer, T., Strugnell, R. A. & other authors (2012). A bioinformatic strategy for the detection, classification and analysis of bacterial autotransporters. *PLoS One* **7**, e43245.

Chen, S. L., Hung, C. S., Xu, J., Reigstad, C. S., Magrini, V., Sabo, A., Blasiar, D., Bieri, T., Meyer, R. R. & other authors (2006). Identification of genes subject to positive selection in uropathogenic strains of *Escherichia coli*: a comparative genomics approach. *Proc Natl Acad Sci U S A* **103**, 5977–5982.

Cota, E., Jones, C., Simpson, P., Altroff, H., Anderson, K. L., du Merle, L., Guignot, J., Servin, A., Le Bouguénec, C. & other authors (2006). The solution structure of the invasive tip complex from Afa/Dr fibrils. *Mol Microbiol* **62**, 356–366.

Danese, P. N., Pratt, L. A., Dove, S. L. & Kolter, R. (2000). The outer membrane protein, antigen 43, mediates cell-to-cell interactions within *Escherichia coli* biofilms. *Mol Microbiol* **37**, 424–432.

Diderichsen, B. (1980). *flu*, a metastable gene controlling surface properties of *Escherichia coli*. *J Bacteriol* **141**, 858–867.

Eto, D. S., Sundsbak, J. L. & Mulvey, M. A. (2006). Actin-gated intracellular growth and resurgence of uropathogenic *Escherichia coli*. *Cell Microbiol* **8**, 704–717.

Fang, L., Nowicki, B. & Yallampalli, C. (2001). Differential expression of uterine NO in pregnant and nonpregnant rats with intrauterine bacterial infection. *Am J Physiol Regul Integr Comp Physiol* **280**, R1356–R1363.

Foxman, B. (1990). Recurring urinary tract infection: incidence and risk factors. *Am J Public Health* **80**, 331–333.

Foxman, B. (2002). Epidemiology of urinary tract infections: incidence, morbidity, and economic costs. *Am J Med* **113** (Suppl 1A), 5–13.

Foxman, B. & Brown, P. (2003). Epidemiology of urinary tract infections: transmission and risk factors, incidence, and costs. *Infect Dis Clin North Am* **17**, 227–241.

Foxman, B., Zhang, L., Tallman, P., Palin, K., Rode, C., Bloch, C., Gillespie, B. & Marrs, C. F. (1995). Virulence characteristics of *Escherichia coli* causing first urinary tract infection predict risk of second infection. *J Infect Dis* **172**, 1536–1541.

Frazier, C. L., San Filippo, J., Lambowitz, A. M. & Mills, D. A. (2003). Genetic manipulation of *Lactococcus lactis* by using targeted group II introns: generation of stable insertions without selection. *Appl Environ Microbiol* **69**, 1121–1128.

Gabrielson, J., Hart, M., Jarelöv, A., Kühn, I., McKenzie, D. & Möllby, R. (2002). Evaluation of redox indicators and the use of digital scanners and spectrophotometer for quantification of microbial growth in microplates. *J Microbiol Methods* **50**, 63–73.

Garcia, M. I., Jouve, M., Nataro, J. P., Gounon, P. & Le Bouguénec, C. (2000). Characterization of the AfaD-like family of invasins encoded by pathogenic *Escherichia coli* associated with intestinal and extra-intestinal infections. *FEBS Lett* **479**, 111–117.

Goluszko, P., Popov, V., Selvarangan, R., Nowicki, S., Pham, T. & Nowicki, B. J. (1997a). Dr fimbriae operon of uropathogenic *Escherichia coli* mediate microtubule-dependent invasion to the HeLa epithelial cell line. *J Infect Dis* **176**, 158–167.

Goluszko, P., Moseley, S. L., Truong, L. D., Kaul, A., Williford, J. R., Selvarangan, R., Nowicki, S. & Nowicki, B. J. (1997b). Development of experimental model of chronic pyelonephritis with *Escherichia coli* O75 : K5:H-bearing Dr fimbriae: mutation in the dra region prevented tubulointerstitial nephritis. *J Clin Invest* **99**, 1662–1672.

Goluszko, P., Niesel, D., Nowicki, B., Selvarangan, R., Nowicki, S., Hart, A., Pawelczyk, E., Das, M., Urvil, P. & Hasan, R. (2001). Dr operon-associated invasiveness of *Escherichia coli* from pregnant patients with pyelonephritis. *Infect Immun* **69**, 4678–4680.

Hasman, H., Chakraborty, T. & Klemm, P. (1999). Antigen-43-mediated autoaggregation of *Escherichia coli* is blocked by fimbriation. *J Bacteriol* **181**, 4834–4841.

Henderson, I. R. & Nataro, J. P. (2001). Virulence functions of autotransporter proteins. *Infect Immun* **69**, 1231–1243.

Henderson, I. R., Meehan, M. & Owen, P. (1997). Antigen 43, a phase-variable bipartite outer membrane protein, determines colony morphology and autoaggregation in *Escherichia coli* K-12. *FEMS Microbiol Lett* **149**, 115–120.

Henderson, I. R., Cappello, R. & Nataro, J. P. (2000). Autotransporter proteins, evolution and redefining protein secretion. *Trends Microbiol* **8**, 529–532.

Henderson, I. R., Navarro-Garcia, F., Desvaux, M., Fernandez, R. C. & Ala'Aldeen, D. (2004). Type V protein secretion pathway: the autotransporter story. *Microbiol Mol Biol Rev* **68**, 692–744.

Johnson, J. R. (1991). Virulence factors in *Escherichia coli* urinary tract infection. *Clin Microbiol Rev* **4**, 80–128.

Jouve, M., Garcia, M. I., Courcoux, P., Labigne, A., Gounon, P. & Le Bouguénec, C. (1997). Adhesion to and invasion of HeLa cells by pathogenic *Escherichia coli* carrying the *afa-3* gene cluster are mediated by the AfaE and AfaD proteins, respectively. *Infect Immun* **65**, 4082–4089.

Justice, S. S., Hung, C., Theriot, J. A., Fletcher, D. A., Anderson, G. G., Footer, M. J. & Hultgren, S. J. (2004). Differentiation and developmental pathways of uropathogenic *Escherichia coli* in urinary tract pathogenesis. *Proc Natl Acad Sci U S A* **101**, 1333–1338.

Kajava, A. V. & Steven, A. C. (2006). The turn of the screw: variations of the abundant beta-solenoid motif in passenger domains of Type V secretory proteins. *J Struct Biol* **155**, 306–315.

Kajava, A. V., Cheng, N., Cleaver, R., Kessel, M., Simon, M. N., Willery, E., Jacob-Dubuisson, F., Locht, C. & Steven, A. C. (2001). Beta-helix model for the filamentous haemagglutinin adhesin of *Bordetella pertussis* and related bacterial secretory proteins. *Mol Microbiol* **42**, 279–292.

Klemm, P. & Schembri, M. A. (2000). Bacterial adhesins: function and structure. *Int J Med Microbiol* **290**, 27–35.

Klemm, P., Hjerrild, L., Gjermansen, M. & Schembri, M. A. (2004). Structure-function analysis of the self-recognizing Antigen 43 autotransporter protein from *Escherichia coli*. *Mol Microbiol* **51**, 283–296.

Le Bouguénec, C. & Servin, A. L. (2006). Diffusely adherent *Escherichia coli* strains expressing Afa/Dr adhesins (Afa/Dr DAEC): hitherto unrecognized pathogens. *FEMS Microbiol Lett* **256**, 185–194.

McCluskey, C., Quinn, J. P. & McGrath, J. W. (2005). An evaluation of three new-generation tetrazolium salts for the measurement of respiratory activity in activated sludge microorganisms. *Microb Ecol* **49**, 379–387.

Mobley, H. L., Green, D. M., Trifillis, A. L., Johnson, D. E., Chippendale, G. R., Lockatell, C. V., Jones, B. D. & Warren, J. W. (1990). Pyelonephritogenic *Escherichia coli* and killing of cultured human renal proximal tubular epithelial cells: role of hemolysin in some strains. *Infect Immun* **58**, 1281–1289.

Mulvey, M. A., Schilling, J. D. & Hultgren, S. J. (2001). Establishment of a persistent *Escherichia coli* reservoir during the acute phase of a bladder infection. *Infect Immun* **69**, 4572–4579.

Mysorekar, I. U. & Hultgren, S. J. (2006). Mechanisms of uropathogenic *Escherichia coli* persistence and eradication from the urinary tract. *Proc Natl Acad Sci U S A* **103**, 14170–14175.

Nowicki, B., Barrish, J. P., Korhonen, T., Hull, R. A. & Hull, S. I. (1987). Molecular cloning of the *Escherichia coli* O75X adhesin. *Infect Immun* **55**, 3168–3173.

Nowicki, B., Truong, L., Moulds, J. & Hull, R. (1988). Presence of the Dr receptor in normal human tissues and its possible role in the pathogenesis of ascending urinary tract infection. *Am J Pathol* **133**, 1–4.

Nowicki, B., Svanborg-Edén, C., Hull, R. & Hull, S. (1989). Molecular analysis and epidemiology of the Dr hemagglutinin of uropathogenic *Escherichia coli*. *Infect Immun* **57**, 446–451.

Nowicki, B., Fang, L., Singhal, J., Nowicki, S. & Yallampalli, C. (1997). Lethal outcome of uterine infection in pregnant but not in nonpregnant rats and increased death rate with inhibition of nitric oxide. *Am J Reprod Immunol* **38**, 309–312.

Nowicki, B., Singhal, J., Fang, L., Nowicki, S. & Yallampalli, C. (1999). Inverse relationship between severity of experimental pyelonephritis and nitric oxide production in C3H/HeJ mice. *Infect Immun* **67**, 2421–2427.

Nowicki, B., Selvarangan, R. & Nowicki, S. (2001). Family of *Escherichia coli* Dr adhesins: decay-accelerating factor receptor recognition and invasiveness. *J Infect Dis* **183** (Suppl 1), S24–S27.

Oelschlaeger, T. A., Dobrindt, U. & Hacker, J. (2002). Pathogenicity islands of uropathogenic *E. coli* and the evolution of virulence. *Int J Antimicrob Agents* **19**, 517–521.

Owen, P. & Kaback, H. R. (1978). Molecular structure of membrane vesicles from *Escherichia coli*. *Proc Natl Acad Sci U S A* **75**, 3148–3152.

Owen, P., Meehan, M., de Loughry-Doherty, H. & Henderson, I. (1996). Phase-variable outer membrane proteins in *Escherichia coli*. *FEMS Immunol Med Microbiol* **16**, 63–76.

Perutka, J., Wang, W., Goerlitz, D. & Lambowitz, A. M. (2004). Use of computer-designed group II introns to disrupt *Escherichia coli* DExH/D-box protein and DNA helicase genes. *J Mol Biol* **336**, 421–439.

Pettit, R. K., Weber, C. A., Kean, M. J., Hoffmann, H., Pettit, G. R., Tan, R., Franks, K. S. & Horton, M. L. (2005). Microplate Alamar blue assay for *Staphylococcus epidermidis* biofilm susceptibility testing. *Antimicrob Agents Chemother* **49**, 2612–2617.

Piątek, R., Zalewska, B., Kolaj, O., Ferens, M., Nowicki, B. & Kur, J. (2005). Molecular aspects of biogenesis of *Escherichia coli* Dr fimbriae: characterization of DraB–DraE complexes. *Infect Immun* **73**, 135–145.

Plançon, L., Du Merle, L., Le Friec, S., Gounon, P., Jouve, M., Guignot, J., Servin, A. & Le Bouguénec, C. (2003). Recognition of the cellular beta1-chain integrin by the bacterial AfaD invasin is implicated in the internalization of *afa*-expressing pathogenic *Escherichia coli* strains. *Cell Microbiol* **5**, 681–693.

Rana, T., Hasan, R. J., Nowicki, S., Venkatarajan, M. S., Singh, R., Urvil, P. T., Popov, V., Braun, W. A., Popik, W. & other authors (2014). Complement protective epitopes and CD55–microtubule complexes facilitate the invasion and intracellular persistence of uropathogenic *Escherichia coli*. *J Infect Dis* **209**, 1066–1076.

Schembri, M. A. & Klemm, P. (2001). Coordinate gene regulation by fimbriae-induced signal transduction. *EMBO J* **20**, 3074–3081.

Schembri, M. A., Kjaergaard, K. & Klemm, P. (2003). Global gene expression in *Escherichia coli* biofilms. *Mol Microbiol* **48**, 253–267.

Servin, A. L. (2005). Pathogenesis of Afa/Dr diffusely adhering *Escherichia coli*. *Clin Microbiol Rev* **18**, 264–292.

Sherlock, O., Schembri, M. A., Reisner, A. & Klemm, P. (2004). Novel roles for the AIDA adhesin from diarrheagenic *Escherichia coli*: cell aggregation and biofilm formation. *J Bacteriol* **186**, 8058–8065.

Ulett, G. C., Valle, J., Beloin, C., Sherlock, O., Ghigo, J. M. & Schembri, M. A. (2007). Functional analysis of antigen 43 in uropathogenic *Escherichia coli* reveals a role in long-term persistence in the urinary tract. *Infect Immun* **75**, 3233–3244.

van der Woude, M. W. & Henderson, I. R. (2008). Regulation and function of Ag43 (*flu*). *Annu Rev Microbiol* **62**, 153–169.

van der Woude, M. W., Braaten, B. A. & Low, D. A. (1992). Evidence for global regulatory control of pilus expression in *Escherichia coli* by Lrp and DNA methylation: model building based on analysis of *pap*. *Mol Microbiol* **6**, 2429–2435.

Van Loy, C. P., Sokurenko, E. V. & Moseley, S. L. (2002). The major structural subunits of Dr and F1845 fimbriae are adhesins. *Infect Immun* **70**, 1694–1702.

Welch, R. A., Burland, V., Plunkett, G. III, Redford, P., Roesch, P., Rasko, D., Buckles, E. L., Liou, S. R., Boutin, A. & other authors (2002). Extensive mosaic structure revealed by the complete genome sequence of uropathogenic *Escherichia coli*. *Proc Natl Acad Sci U S A* **99**, 17020–17024.

Wells, T. J., Totsika, M. & Schembri, M. A. (2010). Autotransporters of *Escherichia coli*: a sequence-based characterization. *Microbiology* **156**, 2459–2469.

Wróblewska-Seniuk, K., Selvarangan, R., Hart, A., Pladzyk, R., Goluszko, P., Jafari, A., duMerle, L., Nowicki, S., Yallampalli, C. & other authors (2005). Dra/AfaE adhesin of uropathogenic Dr/Afa$^+$ *Escherichia coli* mediates mortality in pregnant rats. *Infect Immun* **73**, 7597–7601.

Wróblewska-Seniuk, K., Nowicki, S., Le Bouguénec, C., Nowicki, B. & Yallampalli, C. (2011). Maternal/fetal mortality and fetal growth restriction: role of nitric oxide and virulence factors in intrauterine infection in rats. *Am J Obstet Gynecol* **205**, 83e1–83e7.

Zalewska, B., Piątek, R., Konopa, G., Nowicki, B., Nowicki, S. & Kur, J. (2003). Chimeric Dr fimbriae with a herpes simplex virus type 1 epitope as a model for a recombinant vaccine. *Infect Immun* **71**, 5505–5513.

Zalewska, B., Piątek, R., Bury, K., Samet, A., Nowicki, B., Nowicki, S. & Kur, J. (2005). A surface-exposed DraD protein of uropathogenic *Escherichia coli* bearing Dr fimbriae may be expressed and secreted independently from DraC usher and DraE adhesin. *Microbiology* **151**, 2477–2486.

Zalewska-Piątek, B., Bury, K., Piątek, R., Bruździak, P. & Kur, J. (2008). Type II secretory pathway for surface secretion of DraD invasin from the uropathogenic *Escherichia coli* Dr$^+$ strain. *J Bacteriol* **190**, 5044–5056.

Zalewska-Piątek, B. M., Wilkanowicz, S. I., Piątek, R. J. & Kur, J. W. (2009). Biofilm formation as a virulence determinant of uropathogenic *Escherichia coli* Dr$^+$ strains. *Pol J Microbiol* **58**, 223–229.

Zalewska-Piątek, B., Wilkanowicz, S., Bruździak, P., Piątek, R. & Kur, J. (2013). Biochemical characteristic of biofilm of uropathogenic *Escherichia coli* Dr$^+$ strains. *Microbiol Res* **168**, 367–378.

Zhong, J., Karberg, M. & Lambowitz, A. M. (2003). Targeted and random bacterial gene disruption using a group II intron (targetron) vector containing a retrotransposition-activated selectable marker. *Nucleic Acids Res* **31**, 1656–1664.

Edited by: K. Fields